

Enhancement of Acidic Hydrogen Evolution Reaction Efficiency through Cu/Ni-doped MFI-type Protozeolite Layered Nanoclusters

Xiaodi Zhang¹, Xiyuan Tong^{1#}, Junyang Wang ^{1#}, Xinyu Zhu¹, Zhuozhe Li¹, Fang Fang¹, Kun Qian^{1*}, Yifeng E^{1*}

1. Jinzhou Medical University, Jinzhou 121001, P. R. China.

Submitted to *RSC Advances* as a full paper

Corresponding Author:

Dr. Yifeng E

E-mail: eyf@jzmu.edu.cn

Dr. Kun Qian

E-mail: skyeearth20032003@163.com

#Xiyuan Tong and Junyang Wang contributes equal to Xiaodi Zhang for this work

Table caption

Table S1. Comparison of main element distribution ratio in EDS and XPS.

Table S1. Comparison of main element distribution ratio in EDS and XPS.

Element	Cu	Ni	Na	Al	Si
Method					
EDS (before electroreduction)	0.74%	1.47%	0.1%	0.82%	5.15%
EDS (after electroreduction)	0.2%	0.96%	0.19%	0.24%	18.73%
XPS (before electroreduction)	1.27%	6.66%	—	3.66%	16.9%
XPS (after electroreduction)	0.35%	4.42%	—	2.13%	22.76%

Note: Atom Conc %.

Figure caption

Figure S1. The EDS images for the catalyst (A), Al (B), Na (C), C (D), Si (E), O (F).

Figure S2. The XPS spectra of Al (A), Si (B), C (C) and O (D) in product before electroreduction and the XPS spectra of Al (E), Si (F), C (G) and O (H) in product after electroreduction.

Figure S3. CV of GC (A), MFI-PZ/GC (B), Ni/MFI-PZ/GC (C), Cu/MFI-PZ/GC (D) and Cu/Ni/MFI-PZ/GC (E) measured in a non-Faradaic region at scan rates from 60 to 160 mV s^{-1} in 0.5 M H_2SO_4 . (F) The linear relationship between scan rates and charging currents of Cu/Ni/MFI-PZ/GC (a), Cu/MFI-PZ/GC (b), Ni/MFI-PZ/GC (c), MFI-PZ/GC (d) and GC (e).

Figure S4. LSV of Cu/MFI-PZ/GC (A) and Ni/MFI-PZ/GC (B) were measured before and after A i-t C electroreduction at -1 V in 0.5 M H_2SO_4 for the required time; (C) The relationship between activity time and overpotential of Cu/Ni/MFI-PZ/GC (a), Cu/MFI-PZ/GC (b) and Ni/MFI-PZ/GC (c); LSV plots of Ni/MFI-PZ/GC (D), Cu/MFI-PZ/GC (E) before and after stability test.

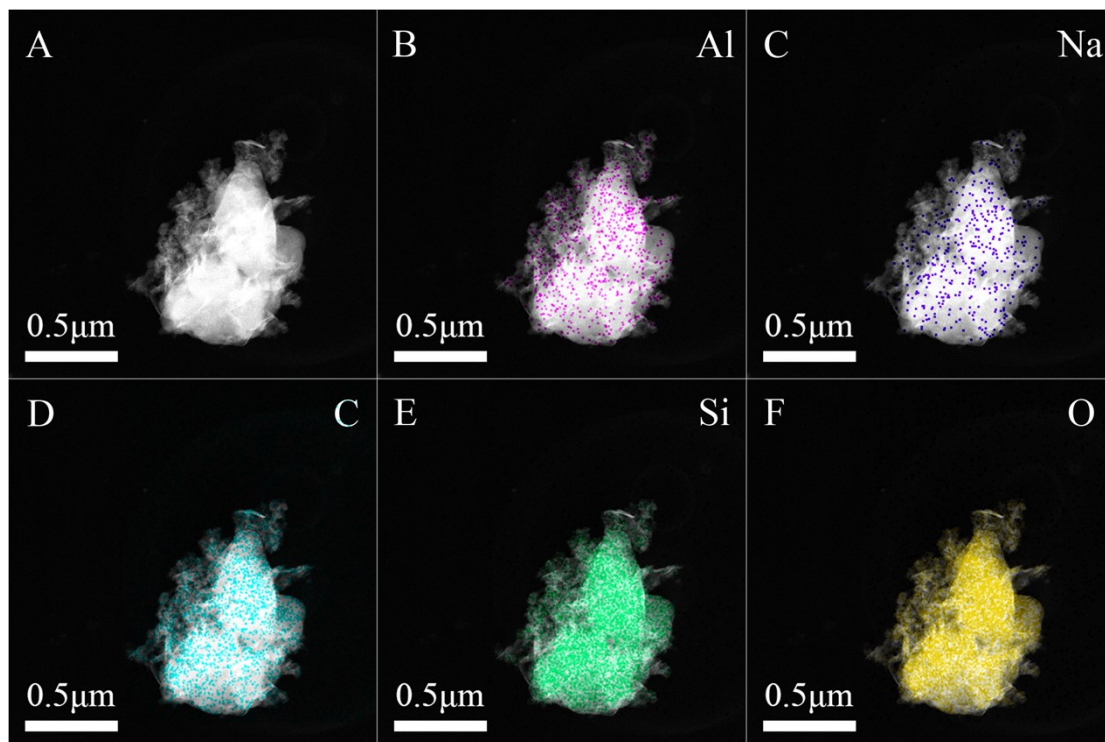


Figure S1. The EDS images for the catalyst (A), Al (B), Na (C), C (D), Si (E), O (F).

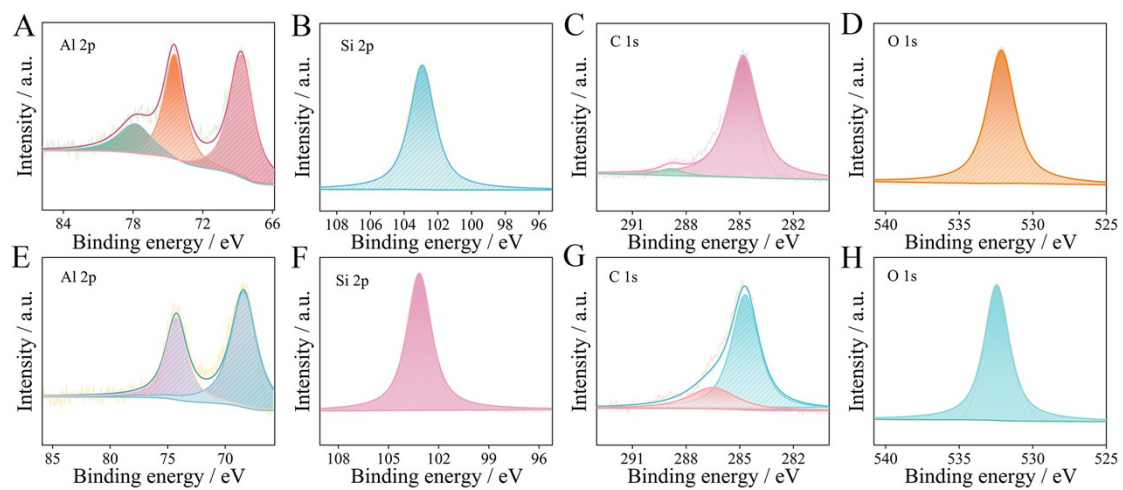


Figure S2. The XPS spectra of Al (A), Si (B), C (C) and O (D) in product before electroreduction. The XPS spectra of Al (E), Si (F), C (G) and O (H) in product after electroreduction.

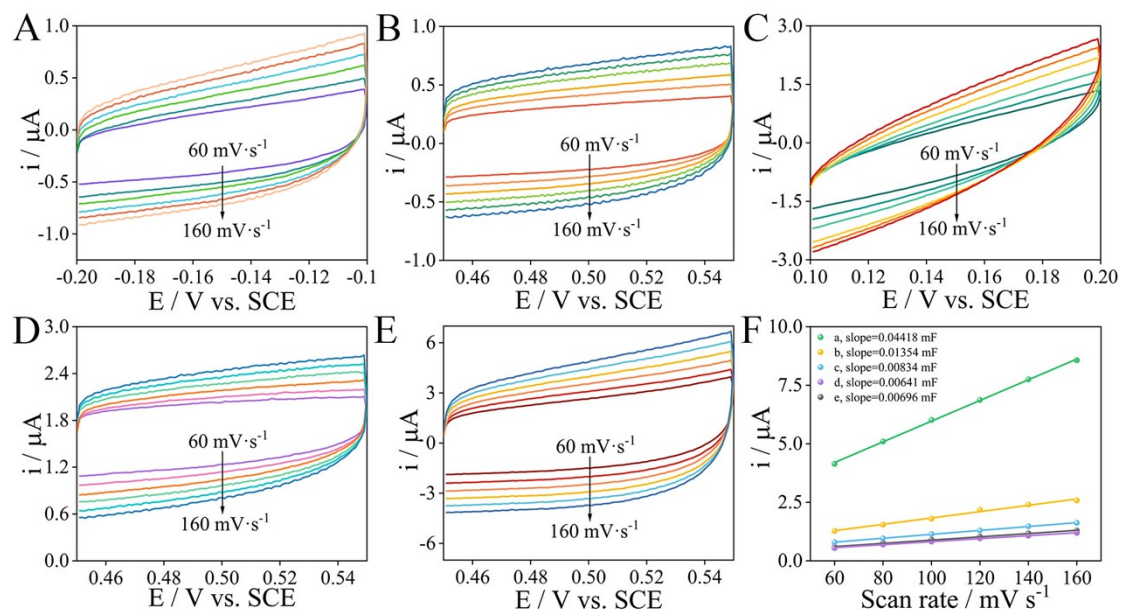


Figure S3. CV of GC (A), MFI-PZ/GC (B), Ni/MFI-PZ/GC (C), Cu/MFI-PZ/GC (D) and Cu/Ni/MFI-PZ/GC (E) measured in a non-Faradaic region at scan rates from 60 to 160 $\text{mV}\cdot\text{s}^{-1}$ in 0.5 M H_2SO_4 . (F) The linear relationship between scan rates and charging currents of Cu/Ni/MFI-PZ/GC (a), Cu/MFI-PZ/GC (b), Ni/MFI-PZ/GC (c), MFI-PZ/GC (d) and GC (e).

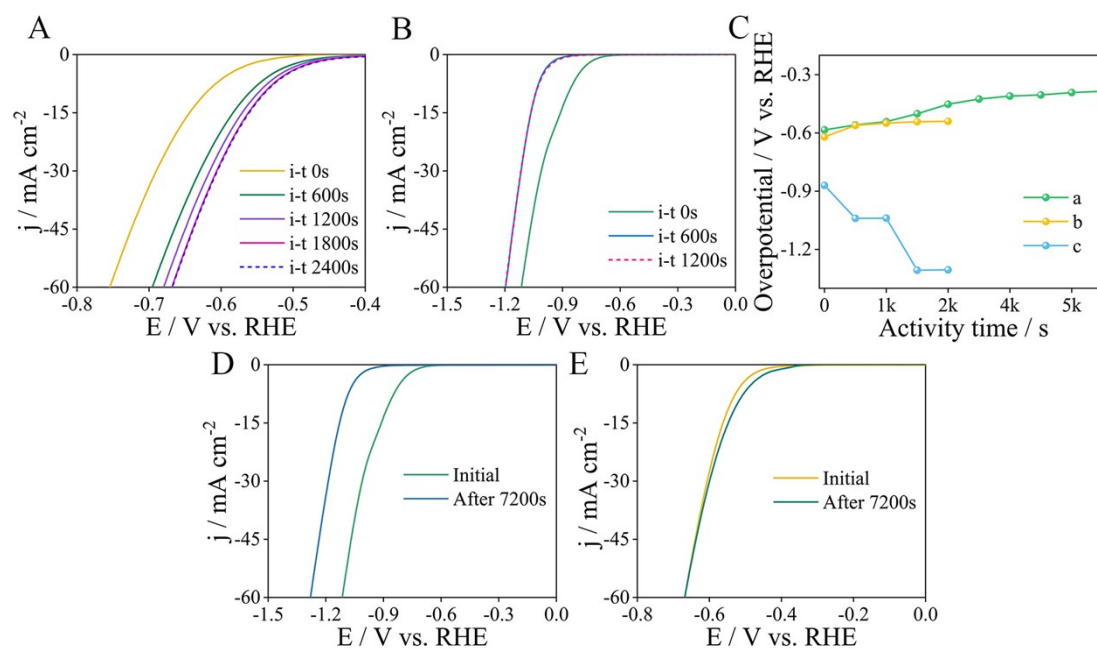


Figure S4. LSV of Cu/MFI-PZ/GC (A) and Ni/MFI-PZ/GC (B) were measured before and after A i-t C electroreduction at -1 V in 0.5 M H₂SO₄ for the required time; (C) The relationship between activity time and overpotential of Cu/Ni/MFI-PZ/GC (a), Cu/MFI-PZ/GC (b) and Ni/MFI-PZ/GC (c); LSV plots of Ni/MFI-PZ/GC (D), Cu/MFI-PZ/GC (E) before and after stability test.